Journal of Maps

ISSN: (Print) 1744-5647 (Online) Journal homepage: http://www.tandfonline.com/loi/tjom20

Solar potential of rooftops in Cáceres city, Spain

Elia Quirós, Mar Pozo & José Ceballos

To cite this article: Elia Quirós, Mar Pozo & José Ceballos (2018) Solar potential of rooftops in Cáceres city, Spain, Journal of Maps, 14:1, 44-51, DOI: 10.1080/17445647.2018.1456487

To link to this article: https://doi.org/10.1080/17445647.2018.1456487

JOURNAL OF MAPS, 2018
VOL. 14, NO. 1, 44–51
https://doi.org/10.1080/17445647.2018.1456487

Taylor & Francis
Taylor & Francis Group

Social Science

Solar potential of rooftops in Cáceres city, Spain

Elia Quirós [a], Mar Pozo[a] and José Ceballos [b]

[a]Department of Graphic Expression, University of Extremadura, Cáceres, Spain; [b]Department of Construction, University of Extremadura, Cáceres, Spain

ABSTRACT

Climate change is one of the challenges our society has to deal with nowadays. Photovoltaic is one of the main renewable energies and it is gaining ground all around the world. The prediction of solar radiation is crucial for this kind of energy. The aim of this work is to produce a solar potential map of rooftops the city of Cáceres (Spain) providing an overview of the employed methodology. The estimation of global radiation is based on LiDAR data of high density. Historical radiation records have been also employed to define the calculation parameters. The representation of the estimated global radiation on each building provides a wide range of new possibilities in the use of renewable energies and changes the conception of rooftops to a potential source of photovoltaic energy.

ARTICLE HISTORY
Received 29 October 2017
Revised 6 March 2018
Accepted 7 March 2018

KEYWORDS
Rooftop solar photovoltaic potential; geographical information system; LiDAR; renewable energy generation; sustainability; building shadow

1. Introduction

The use of renewable energies is one of the most effective tools against climate change. As reported by the International Renewable Energy Agency, at the end of 2016, global renewable generation capacity amounted to 2006 GW. Photovoltaics (PV) and Wind Energy are key technology options for implementing the shift to a decarbonised energy supply and can be deployed in a modular way almost everywhere on this planet (Lacal Arantegui & Jäger-Waldau, 2017).

Policy-makers and investors tend to pay most of their attention to wind and solar electricity, while high-capital baseload technologies like nuclear, coal and natural gas are currently politically and economically less attractive (Paltsev, 2016). Solar energy is abundant, offers significant opportunities for climate change mitigation and it can be used to meet a variety of energy service needs (Hoggett, 2014). The International Energy Agency expects that in the next 5 years 30,000 solar panels will be installed every hour. Their previsions include China, USA and the EU at the top of the growing communities.

More efficient buildings are supporting the whole energy system transformation: Rapid deployment of high-efficiency lighting, cooling and other appliances. Solar building envelopes are increasingly attracting interest (Maurer, Cappel, & Kuhn, 2017). Additionally, urban energy landscapes are generating an urban energy transition towards experimentation in sustainability governance. It has a direct implication not just for planning, but also for the development of energy and urban policy that reflects the fundamental idea that spatial diversity relates to the production of innovation (Broto, 2017).

Recent studies like Bazán, Rieradevall, Gabarrell, and Vázquez-Rowe (2018) support that installing photovoltaic panels in rooftops would allow cities to be self-sufficient in electricity production for residential, commercial and public lighting purposes provided that these investments were to be performed in underutilised rooftops as well as supposes an attractive action in terms of climate change mitigation.

The prediction of solar radiation is crucial for this kind of PV energy, and has been a research topic in recent years and in several locations (Yaniktepe, Kara, & Ozalp, 2017). Usually, this kind of prediction is performed by Geographical Information Systems, but many other applications are being developed for these issues, like: Donatelli, Carlini, and Bellocchi (2006) who developed a software component called *GSRad* containing models to estimate extraterrestrial and ground-level solar radiation; Bezir, Akkurt, and Özek (2010) who proposed another programme that uses altitude, latitude, date and temperature of the place as an input for obtaining both daily and monthly solar radiation; Bayrakçı, Demircan, and Keçebaş (2017) who developed empirical models for estimating global solar radiation on horizontal surface. Moreover there are open access calculators like: Photovoltaic Geographical Information System: European

CONTACT Elia Quirós equiros@unex.es Department of Graphic Expression, Polytechnic School, University of Extremadura, Cáceres E10071, Spain

Commission (2015) an European web interface to produce calculations of solar radiation and PV system energy production; NASA (2016) a Web Mapping Application and Services contain geospatially enabled solar, meteorology and cloud related parameters formulated for assessing and designing renewable energy systems; Energy Sector Management Assistance Program (2016) an interactive atlas that provides long-term averages of solar resource to determine solar power generation; Solargis Company Ltd (2016) which includes a software for making a reliable calculation of PV electricity potential, and within the particular area, Ciemat (2012) have designed an interface called ADRASE that offers solar radiation data, with an approximate resolution of 5 × 5 km.

The aim of this work is to perform a solar potential map of rooftops in Cáceres city (Spain) based on Light Detection and Ranging (LiDAR) data and historical radiation records.

2. Study area and data

2.1. Cáceres city

The studied area is located in western Spain. It is a small city of 36 km^2 with a population of around 100,000. It has a Mediterranean climate with smooth winters and warm summers, in which the average maximum temperature is 34°C. Rainfall is abundant in the months of October, November, March, April and May, but very intermittent.

As shown in Figure 1, Cáceres is positioned in the area with higher solar potential values in Europe, with approximately 5.1 kWh/m^2 of average global radiation in a year.

Constructions are medium sized in a large extent of the city centre, and the abrupt orography of the city is notable. As shown in Figure 2, there are approximately 15,200 buildings distributed along the urban extension, but nearly none of them have solar panels to leverage

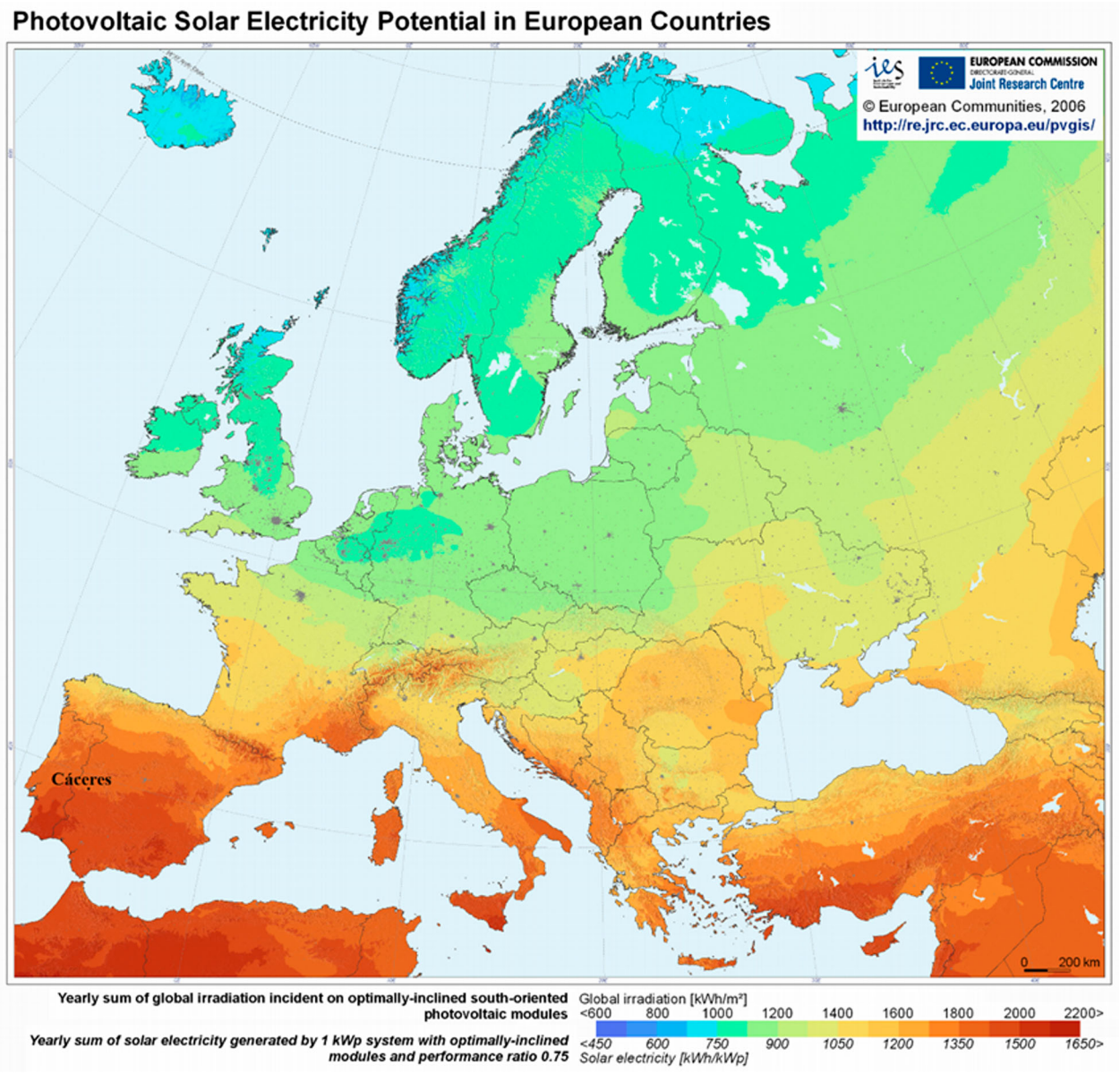

Figure 1. PV solar electricity potential in Europe (Source: http://re.jrc.ec.europa.eu/pvgis/).

Figure 2. Orthophoto of Cáceres city (Source: Google Earth).

the received solar energy, with the exception of some residential houses, that use this energy to warm up their own water tanks.

2.2. LiDAR data and rooftop vectors

LiDAR has been used to record the Earth's surface since the beginning of the 1990s and developed to a reliable and economic recording method due to the development of efficient sensor and computer technology in recent years.

This method uses polar coordinates to relate Global Positioning System and Inertial Measurement Unit systems to survey the ground with high accuracy. Flight path position and orientation are recorded temporarily and spatially at the same time that the laser scanner measures angle and distance to the Earth's surface.

These LiDAR data have been proved to be a helpful tool for the analysis of the solar potential of partial urban sites in several works such as: Tereci, Schneider, Kesten, Strzalka, and Eicker (2009) or Brito, Gomes, Santos, and Tenedório (2012) with cases studies in suburbs of cities, the second one in 538 identified buildings of Lisbon; Szabó et al. (2016) that compared results of radiation with LiDAR and low-cost drone 3D model in 7 km^2 of urban area and Brito, Freitas, Guimarães, Catita, and Redweik (2017) modelling the radiation of two representative areas of 500×500 m^2.

The airborne laser scanner survey of the area was performed by means of an ASL50-83 survey flight with an average point density of 1.5 pts/m^2. A total of 102,987,890 measured points were obtained to generate the surface model of the city. The vertical accuracy of the obtained point cloud was of ±0.081 m (RMSE).

Additionally, a regular Digital Surface Model (DSM) of 1 m of spatial resolution, generated from the elevation of LiDAR points (Figure 3), was also provided. This raster DSM denotes the eminent differences in elevation between different spaces of the urban area.

The rooftop vectors representing buildings of the city (Figure 4) were obtained by means of photogrammetric techniques from digital images of 9 cm of pixel spatial resolution and a flight scale of 1:3500. Both LiDAR data and rooftop vectors were provided by the local council administration.

2.3. Historical radiation data

An historical series of radiation data was provided by the Spanish Meteorological Agency (AEMET). Daily Global radiation of years 2013, 2014, 2015 and 2016 of the city meteorological station was used for the determination of some crucial parameters of the calculation such as Transmittivity (T) and diffuse proportion (DP).

3. Methods

The solar radiation was calculated in a Geographic Information System (GIS) and based on methods from the hemispherical viewshed algorithm developed

Figure 3. Digital surface model of 1 m of spatial resolution.

Figure 4. Vector rooftops of a residential part of the city.

by Hetrick, Rich, Barnes, and Weiss (1993) and further extended by Fu and Rich (1999, 2000a, 2000b).

This algorithm presumes that solar radiation travels through the atmosphere; later on, it is modified by topography and other surface features, and finally, it is intercepted as direct, diffuse and reflected insolation components. Reflected radiation has to be considered only in places where ground surfaces have high albedo, for example, snow-covered surfaces (Fu & Rich, 1999). As it is not the case, in our study area global radiation has to be calculated only as the sum of direct and diffuse radiation.

3.1. Estimation of calculation parameters

The algorithm used does not model clouds inherently, because clouds are extremely hard to model or predict. However, the hypothetical effects of clouds could be reflected inherently with the transmittivity and DP parameters. Their values are crucial to obtain realistic radiation results of the studied area.

3.1.1. Transmittivity

Solar radiation that reaches at the Earth's surface is only a percentage of the radiation received outside the atmosphere. As stated in Fu and Rich (2000b), Transmittivity is the ratio of the directly transmitted radiation incident on the surface after passing through the unit thickness of the atmosphere to the radiation that would be incident on the surface if the radiation had passed through a vacuum. In other words; Transmittivity is the ratio of the energy reaching the Earth's surface to that which is received at the upper limit of the atmosphere (extraterrestrial). Values range from 0 (no transmission) to 1 (complete transmission).

If the values of the direct, diffuse and global radiation are known, the transmittivity (T) can be obtained using the following equation defined by Galán, Arce, Koch, and Lara (2015):

$$T = \frac{\mathrm{GR}}{\mathrm{ER}}, \tag{1}$$

where GR is the global radiation and ER is the extraterrestrial radiation. The extraterrestrial radiation depends on the latitude (LAT) and the declination (DEC), and it was defined by (Duffie & Beckman, 2013):

$$\mathrm{ER} = \frac{24 \times 3600 G_{\mathrm{SC}}}{\pi}\left(1 + 0.33\cos\frac{360n}{365}\right) \times \left(\cos \mathrm{LAT}\cos \mathrm{DEC}\sin\omega_{\mathrm{s}} + \frac{\pi\omega_{\mathrm{s}}}{180}\sin \mathrm{LAT}\sin \mathrm{DEC}\right), \tag{2}$$

where GSC is the solar constant, n is number of the mid-month day, ω_s is the sunset hour angle and it is defined by Equation (3):

$$\omega_s = -\tan \mathrm{LAT} \tan \mathrm{DEC}. \quad (3)$$

Following the above-described formulas, T was calculated for years 2013, 2014, 2015 and 2016.

3.1.2. Diffuse proportion

The DP is the fraction of radiation that has been scattered over all parts of the sky. This parameter encloses information about atmospheric turbidity: low values being associated with clean skies, and high values of diffuse fraction being linked to high turbidity (Batlles et al., 2008). Values range from 0 to 1. This value should be set according to atmospheric conditions by the following equation, described in Galán et al. (2015):

$$\mathrm{DP} = \frac{\mathrm{GR} - \mathrm{DR}}{\mathrm{GR}}, \quad (4)$$

where GR is the global radiation and DR is the direct radiation.

As in the previous parameter, the DP was calculated for years 2013, 2014, 2015 and 2016.

3.1.3. Other parameters

Two possible diffuse models have to be selected for the calculation. On the one hand, Uniform Overcast Sky (UOS), which is often applied in clear sky conditions (non-rainy months). This model assumes that the incoming diffuse radiation is the same from all sky directions. On the other hand, in a Standard Overcast (SO) diffuse model, diffuse radiation flux varies with zenith angle. It has a uniform component plus another component that increases towards the zenith (Kennelly & Stewart, 2014).

3.2. Calibration of calculation parameters

Once all the parameters were calculated for each year, the final calculation parameters were obtained as the average of the obtained parameters.

With those averaged parameters, an initial calibration was performed in order to calculate the adjustment between the modelled radiation and the registered global radiation at the AEMET meteorological station for each year.

3.3. Estimation of solar potential of rooftops

Once all the parameters were calibrated, the estimation of solar potential of the whole city was attained. The calculations were performed by means of ArcMap toolbox for solar radiation. Initially, the solar radiation was calculated throughout the whole DSM, in order to obtain real radiation with all the solar hidings produced by trees, other higher buildings, etc.

Finally, the obtained monthly rasters were trimmed off to consider only the rooftops of the city. Monthly quantification of all roofs was assessed and the final radiation map was designed, representing the average radiation in a year.

4. Results

4.1. Estimation of calculation parameters

Firstly, the extraterrestrial radiation was obtained (Table 2) based on Equation (2).

From values in Tables 1 and 2 and Equations (1), (3) and (4), the values of monthly T and DP were calculated for each year and their average was considered as the final estimated parameters for the solar calculation (Table 3).

4.2. Calibration of calculation parameters

The differences between the registered radiation, at the official meteorological station, and the global radiation, calculated with the estimated parameters, can be observed in Figure 5. It can be noticed, on the one hand, a high fitting in non-rainy moths and on the other hand, that calculated radiation in winter months is lower than the registered one, especially from November to February. The obtained results are in

Table 1. Diffuse, direct and global observed radiation in Cáceres meteorological station.

	2013			2014			2015			2016		
	Diffuse	Direct	Global	Diffuse	Direct	Global	Diffuse	Direct	Global	Diffuse	Direct	Global
January	883	1194	2078	974	920	1894	798	1666	2464	1005	700	1705
February	1083	2483	3567	1323	1242	2564	1238	2255	3493	1221	1813	3034
March	1736	1544	3281	1593	2964	4557	1255	3503	4758	1523	3182	4705
April	1881	4289	6169	2039	3633	5671	2197	3293	5489	2195	3158	5352
May	2092	5064	7156	1963	5459	7423	1953	5589	7542	2483	3713	6196
June	1814	6072	7886	1994	5931	7925	2025	5508	7534	1725	6476	8201
July	–	–	–	1625	6196	7821	1504	6753	8257	1546	6417	7963
August	1361	5819	7181	1298	5896	7194	1799	5321	7121	1237	6119	7356
September	1694	3728	5422	1749	2920	4668	1504	4250	5754	1338	4561	5900
October	1553	2050	3603	1451	2222	3672	1589	1561	3150	1353	2499	3852
November	989	1869	2858	1319	897	2216	804	2167	2971	919	1557	2476
December	794	1317	2111	740	1446	2186	1022	781	1803	798	1340	2137

Note: Values in Wh/m^2.

Table 2. Extraterrestrial radiation in Cáceres.

	Extraterrestrial Rad.
January	15,378
February	20,627
March	27,397
April	34,413
May	39,330
June	41,320
July	40,264
August	36,258
September	29,889
October	22,581
November	16,590
December	13,941

Note: Values in Wh/m^2.

substantial agreement with Agugiaro et al. (2012), especially in the underestimated radiation in winter.

From an annual assessment of the accuracy, as shown in Table 4, the minimum differences represent dissimilarities in a day of only 10 Wh/m^2 (year 2014). Contrarily, the worst adjustment is of 0.85 h in a day (year 2015).

4.3. Estimation of solar potential of rooftops

Low carbon technologies are an important element of strategies to mitigate climate change, and diffusion of renewable energies for electricity generation potentially plays an important role within such strategies (Fischer, 2012).

5. Conclusions

In this work, a solar potential map of rooftops in Cáceres city (Spain) has been achieved. The representation of the estimated global radiation on each building provides a wide range of new possibilities in the use of renewable energies and, consequently, it could be of great help in the fight against climate change.

One of the crucial factors of this work is the precision and accuracy of the employed data. There are several studies that use Lidar data for solar modelling like Martínez-Rubio, Sanz-Adan, Santamaría-Peña, and Martínez (2016), Cheng et al. (2018), etc., but using low point density. Some studies like Jia et al. (2013) suggest that point density data set of at least 0.6 pts/m^2 is necessary to generate an accurate digital

Table 3. Estimated calculation parameters.

	T	DP	Diffuse model
January	0.476405	0.449710	SO
February	0.552276	0.384325	SO
March	0.568340	0.353004	SO
April	0.593221	0.366375	UOS
May	0.352899	0.604319	UOS
June	0.271609	0.674908	UOS
July	0.716527	0.194459	UOS
August	0.716143	0.197418	UOS
September	0.654746	0.289075	UOS
October	0.569036	0.416475	SO
November	0.570814	0.383104	SO
December	0.531755	0.407162	SO

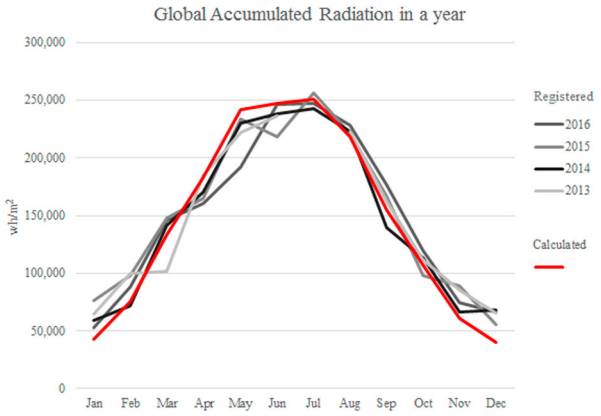

Figure 5. Differences between registered and calculated global radiation in a year at the official meteorological station.

elevation model for the test of the measured urban environment. In this sense, the use of high precision LiDAR data of 1.5 pts/m^2 density confers to the present work a suitable accuracy.

Another major asset of this study is the use of rooftop vectors containing the real roof slopes, as it has been described, obtained by means of photogrammetric techniques with very high precision. These well-defined vectors, avoid the problem detected by Brito et al. (2012) when using only the LiDAR point cloud to define the edges of the roofs.

Additionally, the adoption of historical radiation records to configure the parameters of the calculations, confer the resulting map a pronounced accuracy and a proper fitting with real historical radiation data (an under estimation of less than an hour of energy in a day). In this way, the data and methodology calibration complies with one of the most important requirements stablished by Sergio, Deborah, and Daniel (2017) concerning the obtained result (final map) as a resource for PV decision-making policies.

Finally, focusing on the data obtained, the monthly radiation results in some of the buildings, in months like May, June and July, amounts to more than 7 kWh/m^2. These results suggest that the city has a great renewable energy potential. Changing the perception of rooftops as a potential PV source would have huge consequences for renewable energy policy. Our map can inform decisions concerning PV panels. It can assist the siting of panels on roofs or even gables with optimum inclination, orientation and with no shadows from surrounding elements like buildings or urban vegetation.

Table 4. Differences between calculated values and observed radiation for each year.

Year	Difference in a day (Wh/m^2)	Equivalence in hours
2013	−134	−0.69
2014	−10	−0.05
2015	−179	−0.85
2016	−112	−0.55

Software

Microsoft Excel® 2013 and ESRI® ArcGIS® 10.4 were used to design maps, as well as to obtain radiation values with solar tools.

Acknowledgements

The authors thank both the Local Council GIS Service of Cáceres and the Spanish National Meteorological Agency AEMET for providing the data and for their continued assistance. They also would like to thank the editors and the anonymous reviewers for their careful revision of our manuscript and for their comments and suggestions, which greatly helped to improve the quality of the work.

Disclosure statement

No potential conflict of interest was reported by the authors.

Funding

This work was supported by the Government of Extremadura (Spain) and co-funded by the European Regional Development Fundation under Grant [Project GR15129].

ORCID

Elia Quirós http://orcid.org/0000-0002-8429-045X
José Ceballos http://orcid.org/0000-0002-9951-4751

References

Agugiaro, G., Nexa, F., Remondino, F., Filippi, R. D., Droghetti, S., & Furlanello, C. (2012). *Solar radiation estimation on building roofs and web-based solar cadastre*. XXII ISPRS Congress, Melbourne.

Batlles, F. J., Bosch, J. L., Tovar-Pescador, J., Martínez-Durbán, M., Ortega, R., & Miralles, I. (2008). Determination of atmospheric parameters to estimate global radiation in areas of complex topography: Generation of global irradiation map. *Energy Conversion and Management*, *49*(2), 336–345. doi:10.1016/j.enconman.2007.06.012

Bayrakçı, H. C., Demircan, C., & Keçebaş, A. (2017). The development of empirical models for estimating global solar radiation on horizontal surface: A case study. *Renewable and Sustainable Energy Reviews*. doi:10.1016/j.rser.2017.06.082

Bazán, J., Rieradevall, J., Gabarrell, X., & Vázquez-Rowe, I. (2018). Low-carbon electricity production through the implementation of photovoltaic panels in rooftops in urban environments: A case study for three cities in Peru. *Science of The Total Environment*, *622–623*, 1448–1462. doi:10.1016/j.scitotenv.2017.12.003

Bezir, N. C., Akkurt, I., & Özek, N. (2010). The development of a computer program for estimating solar radiation. *Energy Sources, Part A: Recovery, Utilization, and Environmental Effects*, *32*(11), 995–1003. doi:10.1080/15567030902937234

Brito, M. C., Freitas, S., Guimarães, S., Catita, C., & Redweik, P. (2017). The importance of facades for the solar PV potential of a Mediterranean city using LiDAR data. *Renewable Energy*, *111*, 85–94. doi:10.1016/j.renene.2017.03.085

Brito, M. C., Gomes, N., Santos, T., & Tenedório, J. A. (2012). Photovoltaic potential in a Lisbon suburb using LiDAR data. *Solar Energy*, *86*(1), 283–288. doi:10.1016/j.solener.2011.09.031

Broto, V. C. (2017). Energy landscapes and urban trajectories towards sustainability. *Energy Policy*, *108*, 755–764. doi:10.1016/j.enpol.2017.01.009

Cheng, L., Xu, H., Li, S., Chen, Y., Zhang, F., & Li, M. (2018). Use of LiDAR for calculating solar irradiance on roofs and façades of buildings at city scale: Methodology, validation, and analysis. *ISPRS Journal of Photogrammetry and Remote Sensing*, *138*, 12–29. doi:10.1016/j.isprsjprs.2018.01.024

Ciemat. (2012). ADRASE.

Donatelli, M., Carlini, L., & Bellocchi, G. (2006). A software component for estimating solar radiation. *Environmental Modelling & Software*, *21*(3), 411–416. doi:10.1016/j.envsoft.2005.04.002.

Duffie, J. A., & Beckman, W. A. (2013). *Solar engineering of thermal processes*. Madison, WI: Willey.

Energy Sector Management Assistance Program. (2016). Global Solar Atlas.

Fischer, D. (2012). Challenges of low carbon technology diffusion: Insights from shifts in China's photovoltaic industry development. *Innovation and Development*, *2*(1), 131–146. doi:10.1080/2157930X.2012.667210.

Fu, P., & Rich, P. (1999). *Design and implementation of the solar analyst: An ArcView extension for modeling solar radiation at landscape scales. Proceedings of the nineteenth annual ESRI user conference*, Lawrence, KS.

Fu, P., & Rich, P. (2000a). *A geometric solar radiation model and its applications in agriculture and forestry. Proceedings of the second international conference on geospatial information in agriculture and forestry*, Lake Buena Vista, FL.

Fu, P., & Rich, P. (2000b). *The solar analyst user manual*. Lawrence, KS: Helios Environmental Modeling Institute.

Galán, R., Arce, A., Koch, C., & Lara, P. F. A. (eds.). (2015). *Modelo de cuantificación del potencial fotovoltaico de España*, Sevilla, Spain.

Hetrick, W. A., Rich, P. M., Barnes, F. J., & Weiss, S. B. (1993). GIS-based solar radiation flux models. *American Society for photogrammetry and remote sensing, Technical Papers. Vol 3, GIS* (Photogrammetry and Modeling. pp. 132–143).

Hoggett, R. (2014). Technology scale and supply chains in a secure, affordable and low carbon energy transition. *Applied Energy*, *123*, 296–306. doi:10.1016/j.apenergy.2013.12.006

Jia, Y., Lan, T., Peng, T., Wu, H., Li, C., & Ni, G. (2013, July 21–26). *Effects of point density on DEM accuracy of airborne LiDAR. 2013 IEEE international geoscience and remote sensing symposium – IGARSS*, Melbourne, VIC, Australia.

Kennelly, P. J., & Stewart, A. J. (2014). General sky models for illuminating terrains. *International Journal of Geographical Information Science*, *28*(2), 383–406. doi:10.1080/13658816.2013.848985.

Lacal Arantegui, R., & Jäger-Waldau, A. (2017). Photovoltaics and wind status in the European Union after the Paris agreement. *Renewable and Sustainable Energy Reviews*. doi:10.1016/j.rser.2017.06.052

Martínez-Rubio, A., Sanz-Adan, F., Santamaría-Peña, J., & Martínez, A. (2016). Evaluating solar irradiance over facades in high building cities, based on LiDAR

technology. *Applied Energy*, *183*, 133–147. doi:10.1016/j.apenergy.2016.08.163

Maurer, C., Cappel, C., & Kuhn, T. E. (2017). Progress in building-integrated solar thermal systems. *Solar Energy*. doi:10.1016/j.solener.2017.05.065

NASA. (2016). *Surface meteorology and solar energy*. Retrieved from: https://eosweb.larc.nasa.gov/sse/

Paltsev, S. (2016). The complicated geopolitics of renewable energy. *Bulletin of the Atomic Scientists*, *72*(6), 390–395. doi:10.1080/00963402.2016.1240476

Photovoltaic geographical information system: European Commission. (2015). PVgis photovoltaic calculator. 2017.

Sergio, C., Deborah, A. S., & Daniel, M. K. (2017). Rooftop solar photovoltaic potential in cities: How scalable are assessment approaches? *Environmental Research Letters*, *12*(12), 125005.

Solargis Company Ltd. (2016). SOLARGIS pvPlanner.

Szabó, S., Enyedi, P., Horváth, M., Kovács, Z., Burai, P., Csoknyai, T., & Szabó, G. (2016). Automated registration of potential locations for solar energy production with light detection and ranging (LiDAR) and small format photogrammetry. *Journal of Cleaner Production*, *112*, 3820–3829. doi:10.1016/j.jclepro.2015.07.117

Tereci, A., Schneider, D., Kesten, D., Strzalka, A., & Eicker, U. (2009). *Energy saving potential and economical analysis of solar systems in the urban quarter Scharnhauser Park*. *ISES solar world congress 2009: Renewable energy shaping our future*, Johannesburg, South Africa.

Yaniktepe, B., Kara, O., & Ozalp, C. (2017). The global solar radiation estimation and analysis of solar energy: Case study for Osmaniye, Turkey. *International Journal of Green Energy*, 1–9. doi:10.1080/15435075.2017.1329148.